Journal of Applied Polymer Science

# Silver nanowire network embedded in polydimethylsiloxane as stretchable, transparent, and conductive substrates

**JinHoon Kim,[1] Jaeyoon Park,[1]* Unyong Jeong,[2] Jin-Woo Park[1]**
Department of Materials Science and Engineering, Yonsei University, 50 Yonsei-Ro, Seodaemun-Gu, Seoul, 120-749, Korea
Division of Advanced Materials Science, Pohang University of Science and Technology, Pohang, 790-784, Korea
*Present address: LG Display R&D Center, Paju, 413-811, Korea
Correspondence to: J.-W. Park (E-mail: jwpark09@yonsei.ac.kr)

**ABSTRACT:** Highly stretchable transparent conductors where Ag nanowire networks (AgNWs) are reliably embedded into a polydimethylsiloxane (PDMS) substrate are presented. In spite of the weak physical and chemical interaction between Ag nanowires and PDMS, a significantly high transfer efficiency and uniform embedding of AgNW percolation mesh electrodes into PDMS was achieved by simply coating aerogels onto the AgNWs and using water-assisted transfer. By the failure-free transfer and reliable bonding with the substrate, the conductive PDMS with embedded AgNWs that exhibits a sheet resistance ($R_s$) of 15 Ω/sq and 80% optical transmittance ($T$) are reported here. The PDMS films accommodate tensile strains up to 70% and a cyclic strain of 25% for more than 100 cycles, with subsequent $R_s$ values as low as 90 and 27 Ω/sq, respectively. The $T$ of this conductive PDMS is more than 25% higher than that of networks of CNTs, Cu nanowires, and hybrid composites of CNTs and graphene embedded in elastomer films such as PDMS, polyurethane, and Ecoflex. The simple and reproducible fabrication allows the extensive study and optimization of the stretchability of the meanders in terms of humidity, thickness, and substrate. The results provide new insights for designing stretchable electronics. © 2016 Wiley Periodicals, Inc. J. Appl. Polym. Sci. **2016**, *133*, 43830.

**KEYWORDS:** coatings; mechanical properties; nanoparticles; nanowires and nanocrystals; properties and characterization; surfaces and interfaces

Received 1 March 2016; accepted 24 April 2016
**DOI: 10.1002/app.43830**

## INTRODUCTION

Transparent stretchable conductors are essential components of wearable electronics and optoelectronics that detect and transform the physiological phenomena of the human body into digital signals;[1] such devices include transcutaneous and implantable sensors[2–4] and electronic skins with human-interactive components.[5] The wearable electronics are built on transparent stretchable conductors that make the devices conformable to the human body, which is curved in a complex manner; the electronics are thereby subjected to various mechanical operations including bending, twisting, folding, and stretching.[6] On the basis of the pioneering works by Bao *et al.*,[1] Pei *et al.*,[7,8] and Lee *et al.*,[6,9] inorganic materials with stretchable structures such as network and mesh-structured metal nanowires (NWs), carbon nanotubes (CNTs), graphene, and hybrids of these two-dimensional (2D) materials, coated or embedded in an elastomer film, are the most promising candidates for transparent stretchable conductors.[10] However, achieving a high degree of stretchability with excellent transparency without losing conductivity remains a challenge.[11] In this work, we report highly stretchable and transparent conductive films with Ag nanowire networks (AgNWs) embedded in polydimethylsiloxane (PDMS).[9] AgNWs are more conductive and transparent than CNTs and graphene, and PDMS is the most powerful elastomeric substrate for stretchable electronics because of its good biocompatibility, high stretchability, excellent optical properties, and ease of molding at the nanometer scale.[9,12] However, compositing these two excellent materials, AgNWs and PDMS, to fabricate a transparent stretchable conductor was not successful because the PDMS forms weak physical and chemical interactions between the AgNWs as a consequence of its methyl-terminated nature.[9] Hence, several methods of implanting AgNWs into PDMS matrices have been developed, including using a fluorosurfactant or inserting polyurethane adhesion layers.[9,12]

In this study, stretchable AgNWs are reliably transferred into a PDMS substrate. Several major challenges, including failure-free transfer and reliable bonding with the substrate, are addressed. The conventional fabrication process of AgNW-embedded polymer substrates consists of solution-coating the AgNWs onto a

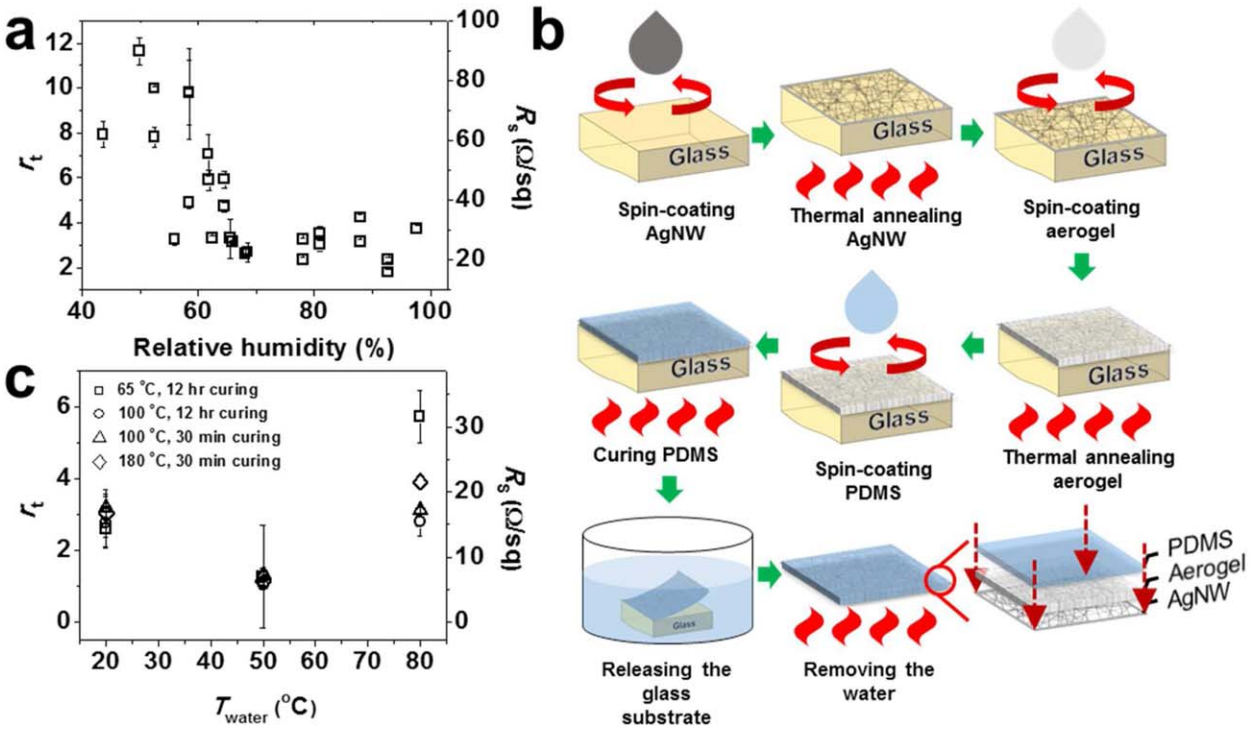


**Figure 1.** (**a**) The effect of the humidity level on the transfer rate of the AgNWs into PDMS, (**b**) schematic description of fabrication process and the structure of the composite electrodes of AgNWs embedded in PDMS, and (**c**) the effects of the water-assisted embedding process parameters on $r_t$ and $R_s$. [Color figure can be viewed in the online issue, which is available at wileyonlinelibrary.com.]

release substrate (glass in this study), casting a polymer onto the AgNWs, and separating the polymer with embedded AgNWs from the release substrate. However, using this common method, AgNWs are not transferred because of their weak physical and chemical interactions with PDMS.[9] Hence, we employed aerogels as a strong transfer medium for incorporating the AgNWs into PDMS. Given the extremely high surface-to-volume ratio of the aerogels, a strong van der Waals interaction is expected among the aerogels, AgNWs, and the PDMS when the aerogels are inserted between the AgNWs and PDMS. This strong interaction is expected to create denser AgNW networks embedded in the PDMS and to promote the detachment of the AgNWs from the release substrate during the embedding process.[9,13]

The AgNWs were transferred into the PDMS with the aerogels; the highest sheet resistance ($R_s$) of the PDMS and the highest ratio between the $R_s$ and that of the AgNWs coated onto glass substrates ($R_{s,0}$) ($r_t$) were 21.6 Ω/sq and 1.77, respectively. When the AgNWs on the glass are perfectly transferred to PDMS, $r_t$ is 1. $r_t$ becomes larger than 1 as less AgNWs is transferred into PDMS. The transfer tests were repeated for more than 6 months because $r_t$ fluctuated substantially, apparently affected by the humidity in the air. Through long testing times, we observed that $r_t$ is almost inversely proportional to the relative humidity in the air measured by a digital hygrometer [Figure 1(a)]. This led us to design the water-assisted process for transferring AgNWs into PDMS. The simple and reproducible fabrication allows the extensive study and optimization of the stretchability of the meanders in terms of humidity, thickness, and substrate. The results provide new insights for designing stretchable electronics.

## EXPERIMENTAL

### Sample Preparation

A 1 wt % AgNW solution (Nanopyxis, Seongnam, Korea) was diluted to 0.25 and 0.5 wt %. The glass substrates were cleaned with acetone, 2-propanol, and deionized water. Diluted AgNW solutions were spin-coated onto the glass substrates at 1000 rpm for 60 sec, and the solvent was evaporated by annealing at 100 °C for 5 min. The AgNWs were then post thermal annealed at 180 °C for 20 min inside an $N_2$-filled glove box. Silica aerogels (JIOS Aerogel Corporation, Osan, Korea) were dispersed into the ethanol at a concentration of 4 wt %. The aerogel was spin-coated at 1000 rpm for 60 sec, followed by annealing at 100 °C for 20 min. PDMS was prepared by mixing the base and the cross linking curing agent (Sylgard 184 elastomer kit from Dow Corning) in a weight ratio of 10:1. The liquid mixture was spin-coated at 400 rpm for 60 sec, and the PDMS was cured at curing temperatures ranging from 65 to 180 °C and for times ranging from 30 min to 12 h. After the PDMS was cured, the composites were dipped into deionized water for 60 min at temperatures ranging from 25 to 80 °C. The composite film was then released from the glass substrate in the water. The composite film was dried at 70 °C for 30 min to remove the residual water.

### OLED Fabrication

OLEDs were fabricated on the composite electrodes. First, the hole transport layer (HTL), PEDOT:PSS (Heraeus, Clevios P VP

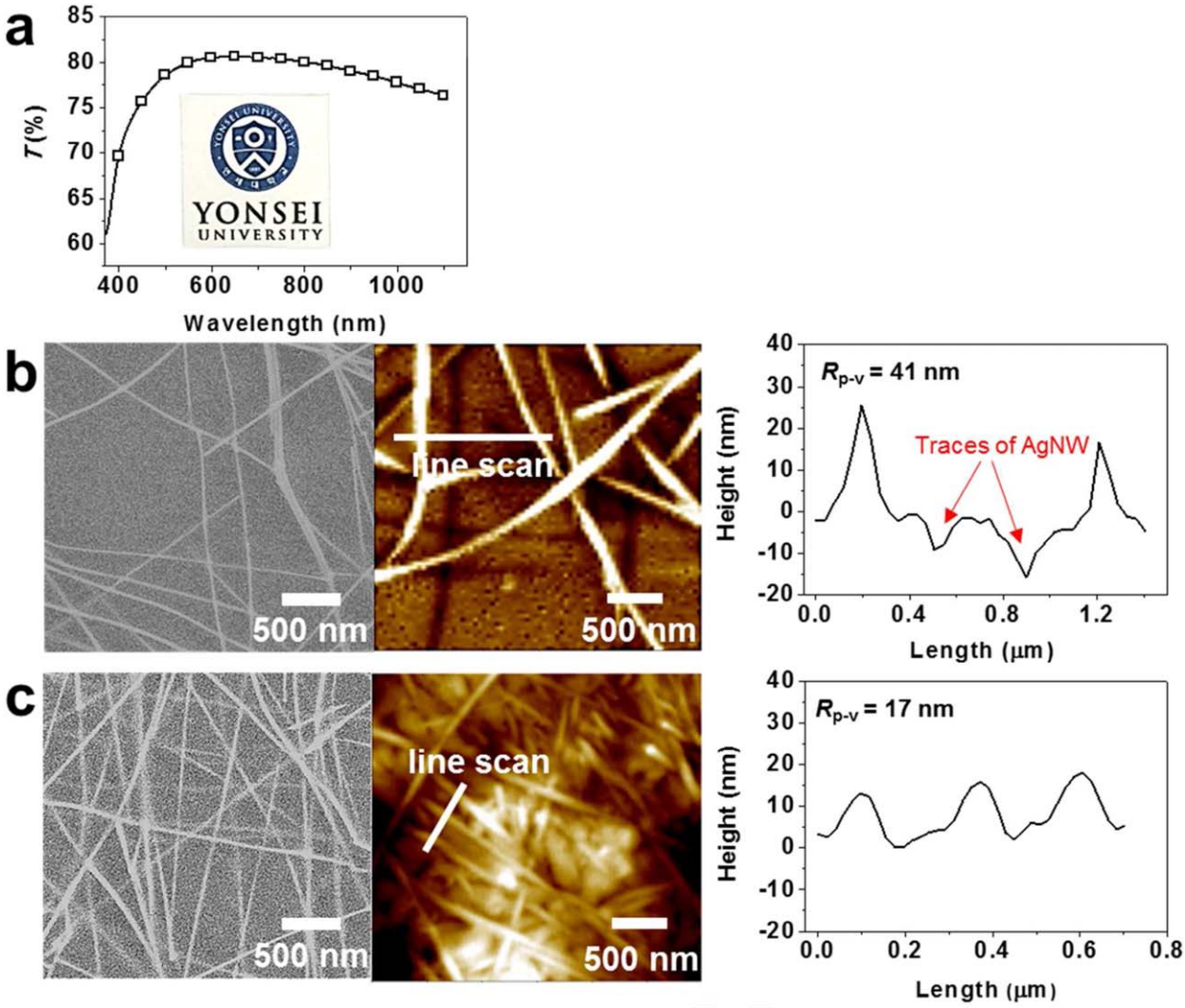


**Figure 2.** (**a**) *T* values of the composite electrode with the inset image of the composite electrode, and FE-SEM (**left**) and AFM (**middle**) images and line scan data across the surfaces (**right**) of the embedded AgNWs in PDMS (**b**) without and (**c**) with aerogels. [Color figure can be viewed in the online issue, which is available at wileyonlinelibrary.com.]

AI 4083), was diluted using 2-propanol at a weight ratio of 1:1. The solution was then stirred at 300 rpm for 3 h and spin-coated at 1000 rpm for 60 sec, followed by a heat treatment at 100 °C for 10 min. A light-emissive layer (EL), SY-PPV (Super-Yellow by Merck), dissolved in toluene (5 mg/mL) was spin-coated onto the HTL at 1500 rpm for 30 sec and then annealed at 100°C for 5 min inside an $N_2$-filled glove box. The electron transport layer (ETL), 0.5 wt % $Cs_2CO_3$ (Sigma-Aldrich) in 2-ethoxyethanol, was spin-coated at 5000 rpm for 30 sec onto the EL and then heat-treated at 100°C for 5 min. Then, the samples were transferred to an evaporator chamber and 150 nm Al films were deposited as the cathode.

### Characterization Tool

The $R_s$ and optical transmittance ($T$) of the composite electrodes were measured using the four-point probe and UV–visible spectroscopy, respectively. The microstructures of the AgNW networks embedded in the PDMS were analyzed using field emission-scanning electron microscopy (FE-SEM), and atomic force microscopy (AFM). The static and cyclic stretching tests of the composite electrodes were performed. In the static stretching test, the strain was applied from 0 to 70%, and the $R_s$ change was measured using four-point probe. The cyclic stretching test was performed at 25% strain at a stretching rate of 16.7% $sec^{-1}$ for 100 cycles, and the $R_s$ was measured in every 20 cycles using four-point probe. The *J–L–V* characteristics of the OLEDs were measured using a Keithley 2400 Sourcemeter and a Minolta CS-200 luminance and color meter.

## RESULTS AND DISCUSSION

Figure 1(b) provides a detailed description of the process of fabricating the PDMS with embedded AgNWs and aerogels. Before the aerogels were coated onto the substrate, the AgNWs on the glass substrate were slightly heated at 180 °C for 20 min inside an $N_2$-filled glove box to weld the junctions of the AgNWs.[14] The PDMS was prepared by mixing the base and cross linking curing agent in a weight ratio of 10:1, and coated on the AgNW

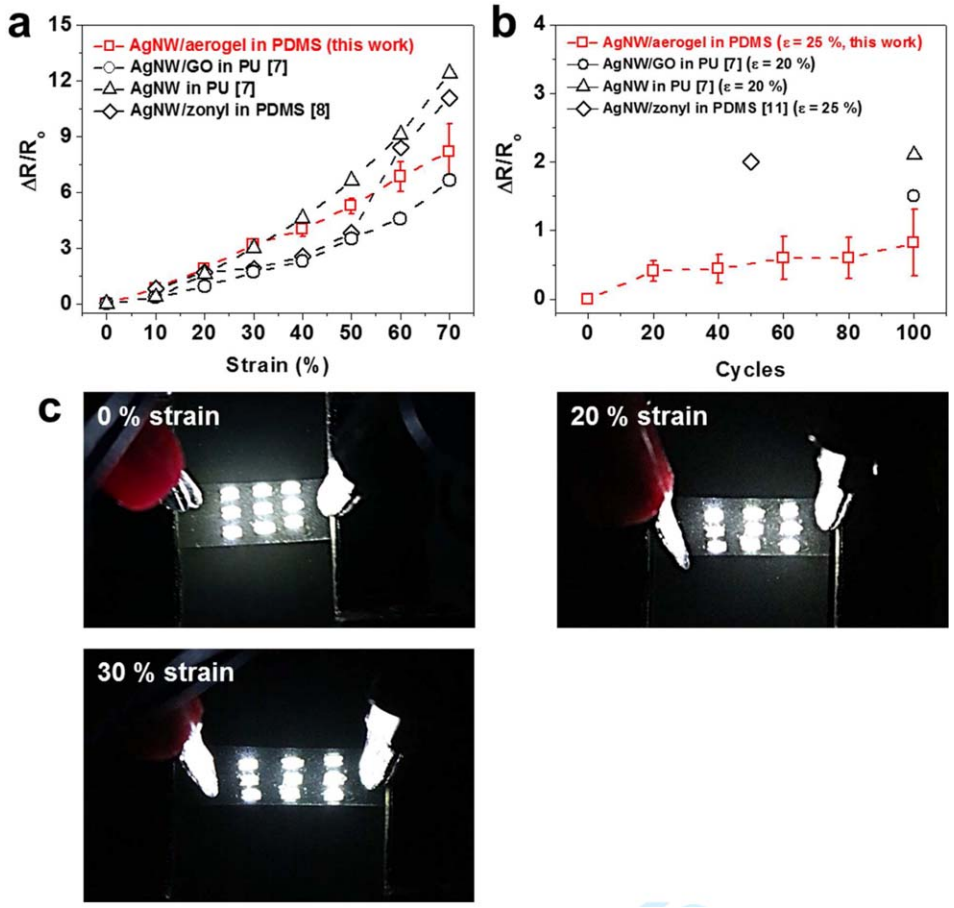


**Figure 3.** (**a**) Static and (**b**) cyclic stretching test results of the composite electrode compared with those of previously reported stretchable electrodes ($\varepsilon$ = strain); (**c**) photographs of $\mu$LEDs mounted onto the composite electrode in flat and stretched states. [Color figure can be viewed in the online issue, which is available at wileyonlinelibrary.com.]

coated glass. The coated liquid mixture was cured at 120 °C for 12 h. The cross linking curing agent contains oligomeric dimethyl siloxane and methyl hydrosiloxane as crosslinking agent and a platinum complex as a catalyst for the hydrosilation reaction.[15] During heat treatment, the curing agent forms cross-links in the polymer chains. As a result, cured PDMS becomes highly elastomeric substrate. The PDMS coated on the release substrate was immersed into a water bath and detached from the substrate; this method is therefore considered to be water-assisted. The final structure of the PDMS with embedded AgNWs and aerogels is also schematically described in Figure 1(b).

According to the experimental results, $r_t$ was not affected by the immersion time in the water, but by the temperature of the water. As shown in Figure 1(c), the average $r_t$ was approximately 1; in addition, the $R_s$ reached its lowest value and was only slightly affected by the curing process conditions when the water temperature was fixed at 50 °C. When the PDMS was cured at 120°C for 12 h and detached from the glass in the 50°C water bath, the $r_t$ was almost one [Figure 1(c)] and the lowest $R_s$ value was 15 Ω/sq. When the PDMS thicknesses was increased from 150 to 250 μm, the observed trends in the variation of the immersion time, water temperature, and curing conditions were similar to the trends in the variation of $r_t$ and $R_s$ in Figure 1(c). A comparison of Figure 1(a–c) reveals that the best $r_t$ became closer to 1—from 1.77 to 1.03—as a result of the water-assisted transfer.

The water-assisted transfer process can be explained from a thermodynamic perspective. Because the release substrate [glass in Figure 1(b)] has a greater affinity for water than for the AgNWs and PDMS,[16] the water will penetrate into and wet the interface between the glass and the PDMS with the embedded AgNWs, leading to the spontaneous separation of the composite electrodes from the glass substrate. The work for the separation ($W_s$) can be estimated by

$$W_s = \left(\gamma_{\text{water - glass}} + \gamma_{\text{water - PDMS}} + \gamma_{\text{water - AgNWs}}\right) - \left(\gamma_{\text{PDMS - glass}} + \gamma_{\text{AgNWs - glass}}\right) \quad (1)$$

where $\gamma_{\text{A-B}}$ denotes the surface tension between A and B. The $W_s$ has been calculated to be −368.19 mJ/m,[17–19] which confirms the spontaneous separation by the water permeation through the interface between the glass and the composite electrode.

The $T$ of the composite electrode within the visible range is plotted in Figure 2(a). The $T$ at 550 nm and the maximum $T$

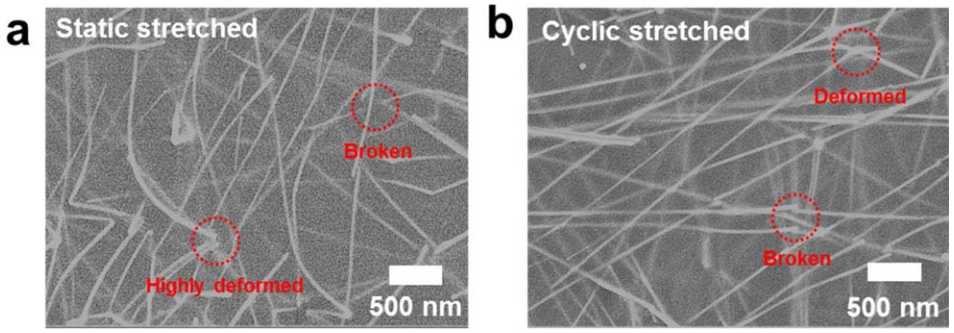


**Figure 4.** The surface analysis results of the embedded electrode after (**a**) static and (**b**) cyclic stretching tests. [Color figure can be viewed in the online issue, which is available at wileyonlinelibrary.com.]

are 79.9 and 80.6%, respectively, which are comparable to commercial indium tin oxide-coated glasses.[20] Also, the $T$ of this conductive PDMS is more than 25% higher than that of networks of CNTs, Cu nanowires, and hybrid composites of CNTs and graphene embedded in elastomer films such as PDMS, polyurethane, and Ecoflex.[10,21] The inset image in Figure 2(a) is a photograph of the composite electrode. Figure 2(b,c) shows the surface microstructures of the embedded AgNWs without and with aerogels, respectively, as analyzed by field-emission scanning electron microscopy (FE-SEM) and atomic force microscopy (AFM). Both electrodes were subjected to water-assisted transfer. In the absence of the aerogels, however, a nonuniform, sparse distribution of AgNWs was observed, as shown in the left FE-SEM image in Figure 2(b). Furthermore, the AFM surface image in the middle of Figure 2(b) shows traces of AgNWs that failed to be embedded, which corresponds to the valleys in the AFM line-scanning data in the right side of Figure 2(b). The diameter of the AgNWs ranged from 25 to 30 nm; however, the average peak-to-valley roughness ($R_{p\text{-}v}$) of the composite surface was 41 nm [right in Figure 2(b)], indicating that the AgNWs are barely attached to the surface of the PDMS.

In our previous work,[13] we showed that aerogels could improve the transfer of AgNWs into a UV-curable polymer [Norland Optical Adhesive 68 (NOA 68)] because of the strong van der Waals interaction of the aerogels with the AgNWs and the matrix. The results in Figure 2(c) correspond well to those of our previous investigations.[13] Contrary to the results in Figure 2(b,c) shows uniformly embedded, dense AgNWs on the surface of the PDMS. According to the AFM results [middle and right images in Figure 2(c)], the $R_{p\text{-}v}$ of the composite electrode with the aerogels is less than half that of the composite electrode without aerogels. This result verifies that the AgNWs are deeply embedded into the PDMS by the aerogels.

To investigate the mechanical stability of the composite electrodes, we performed static and cyclic stretching tests and compared the ratio of the changes in $R_s$ to the original $R_s$ ($\Delta R_s \}R_0^{-1}$) with previously reported results for stretchable electrodes, as shown in Figure 3(a,b).8,9 The PDMS films accommodate tensile strains up to 70% and a cyclic strain of 25% for more than 100 cycles, with subsequent $R_s$ values as low as 90 and 27 Ω/sq, respectively. As shown in Figure 3(a), the $\Delta R_s \}R_0^{-1}$ of the composite electrodes developed in this work almost linearly increases as the strain increases to 70%; the performance of these electrodes is similar to that of electrodes composed of polyurethane (PU) with embedded AgNWs and graphene oxide[8] and better than that of electrodes composed of PDMS with AgNWs embedded with Zonyl FS-300 fluorosurfactant[9] or PU with embedded AgNWs.[8] The cyclic stretchability of the composite electrodes in this work was observed to be superior to those referenced in the static stretching tests. As shown in Figure 3(b), the $\Delta R_s \}R_0^{-1}$ of the PU composite electrode at 20% for 100 cycles[8] and that of PDMS with Zonyl at 25% for 50 cycles[9] are almost two times higher than that of the composite electrode in this study.

Figure 3(c) shows photographs of micro-LEDs (μLEDs) mounted onto the 0, 20, and 30% strained composite films during operation at 7.8 V. The current density and emission intensity of the μLEDs exhibited little change on the strained composite films. The morphological changes in the composite electrodes after static and cyclic stretching tests were analyzed using FE-SEM; the micrographs are shown in Figure 4(a,b), respectively. Figure 4(a) is an FE-SEM image of the composite electrodes stretched by 70% and then released. The fracture of the AgNWs appears to be the reason for the increase in $R_s$ under strain.

Most of the AgNWs are highly deformed and are even folded [Figure 4(a)], which indicates that the adhesion between the AgNWs and polymer matrices was strong and that delamination at the interfaces between the AgNWs and PDMS generally does not occur when stretched and released. AgNWs are known to begin plastic deformation at 1.0–1.5% strain,[22] whereas PDMS deforms elastically until 40% strain.[23,24] The strong adhesion with the PDMS and aerogels appears to retard the strain localization that leads to necking in AgNWs, which enables them to deform without rupture up to very large strains.[25] The FE-SEM image of the cyclically stretched composite electrodes at 25% for 100 cycles [Figure 4(b)] also shows that the AgNWs broke during the tests. Under cyclic strain at 25%, the deformation of the AgNWs [Figure 4(b)] appears to be less severe that at 70% static strain [Figure 4(a)].

Organic light-emitting diodes (OLEDs) were fabricated on the composite electrodes; the schematic description of the OLED structure is shown in Figure 5(a). The current density ($J$)–

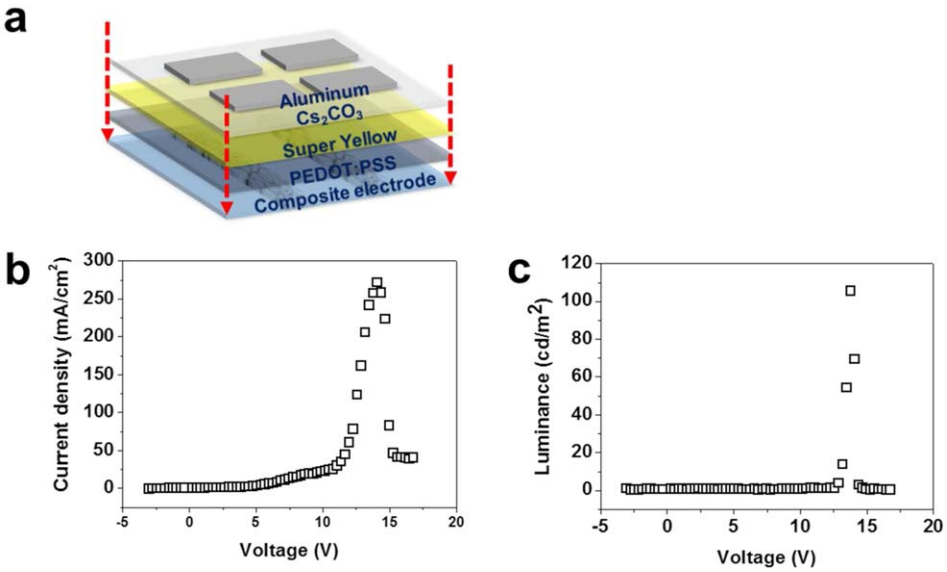


**Figure 5.** (**a**) Schematic descriptions of OLED structures; (**b**) *J–V* curve and (**c**) *L–V* curve of OLEDs fabricated on composite electrodes. [Color figure can be viewed in the online issue, which is available at wileyonlinelibrary.com.]

luminescence (*L*)–voltage (*V*) characteristics of the OLEDs are presented in Figure 5(b,c), respectively. The OLEDs functioned well on the PDMS composite electrodes, as shown in Figure 5(b,c); however, the turn-on voltage ($V_{on}$) at 1 cd/m$^2$ was measured as 12.6 V, which is higher than that of devices fabricated on ITO glass.[26] The high $V_{on}$ of the OLEDs on PDMS is attributable to the contact area between the AgNWs and the semiconducting polymer layer being reduced as the AgNWs are embedded in PDMS[27] and to the hole mobility of the composite electrode being low because of the increased interfacial area.[28] We intend to investigate these issues in future works.

## CONCLUSIONS

We have demonstrated highly stretchable composite electrodes of AgNWs embedded in PDMS; these electrodes exhibit excellent mechanical properties, with a sustained performance under a static mechanical strain up to 70% and cyclic strain to 25% for 100 cycles. The composite electrodes exhibit a good transparency of 80% and a conductivity as low as 15 Ω/sq. A significantly high transfer efficiency and uniform embedding of AgNW percolation mesh electrodes into PDMS was achieved by simply coating aerogels onto the AgNWs and using water-assisted transfer. The aerogels form discontinuously agglomerated particles on the AgNWs; hence, do not affect the flexibility of the AgNWs. This process was made possible by engineering the surfaces of the glass-release substrate, AgNWs, and PDMS with water and aerogels with an extremely large surface-to-volume ratio. The simplicity in the electrode fabrication process provides broad possibilities for further modifications, such as the ease of patterning and integration, improving device performance and incorporating other functionalities.

## ACKNOWLEDGMENTS

This research was supported by the Basic Science Research Program through the National Research Foundation of Korea (NRF), funded by the Ministry of Education (grant number 2015R1D1A1A01061340), and by the Joint Program for Samsung Electronics-Yonsei University.

## REFERENCES

1. Lipomi, D. J.; Vosgueritchian, M.; Tee, B. C. K.; Hellstrom, S. L.; Lee, J. A.; Fox, C. H.; Bao, Z. *Nat. Nanotechnol.* **2011**, *6*, 788.
2. Bansal, A. K.; Hou, S.; Kulyk, O.; Bowman, E. M.; Samuel, I. D. W. *Adv. Mater.* **2015**, *27*, 7638.
3. Lochner, C. M.; Khan, Y.; Pierre, A.; Arias, A. C. *Nat. Commun.* **2014**, *5*, 5745.
4. Pang, C.; Lee, C.; Suh, K. Y. *J. Appl. Polym. Sci.* **2013**, *130*, 1429.
5. Someya, T.; Kato, Y.; Sekitani, T.; Iba, S.; Noguchi, Y.; Murase, Y.; Kawaguchi, H.; Sakurai, T. *Proc. Natl. Acad. Sci. U.S.A.* **2005**, *102*, 12321.
6. Wang, J.; Yan, C.; Cai, G.; Cui, M.; Lee-Sie Eh, A.; See Lee, P. *Adv. Mater.* **2015**, *27*, 2876.
7. Yu, Z. B.; Niu, X. F.; Liu, Z. T.; Pei, Q. B. *Adv. Mater.* **2011**, *23*, 3989.
8. Liang, J. J.; Li, L.; Tong, K.; Ren, Z.; Hu, W.; Niu, X. F.; Chen, Y. S.; Pei, Q. B. *ACS Nano* **2014**, *8*, 1590.
9. Wang, J.; Yan, C.; Kang, W.; Lee, P. S. *Nanoscale* **2014**, *6*, 10734.
10. Yao, S.; Zhu, Y. *Adv. Mater.* **2015**, *27*, 1480.
11. Ahn, S.; Choe, A.; Park, J.; Kim, H.; Son, J. G.; Lee, S. S.; Park, M.; Ko, H. *J. Mater. Chem. C* **2015**, *3*, 2319.
12. Kim, D. H.; Yu, K. C.; Kim, Y.; Kim, J. W. *ACS Appl. Mater. Interfaces* **2015**, *7*, 15214.
13. Kim, J. H.; Park, J. W. *ACS Appl. Mater. Interfaces* **2015**, *7*, 18574.

14. Coskun, S.; Selen Ates, E.; Emrah Unalan, H. *Nanotechnology* **2013**, *24*,
15. Efimenko, K.; Wallace, W. E.; Genzer, J. *J. Colloid Interface Sci.* **2002**, *254*, 306.
16. Wu, S. Polymer Interface and Adhesion; Taylor & Francis: New York, **1982**. p 589.
17. Wang, Z.; Xing, R.; Yu, X.; Han, Y. *Nanoscale* **2011**, *3*, 2663.
18. Vicente, C. M. S.; André, P. S.; Ferreira, R. A. S. *Rev. Bras. Ensino Fís.* **2012**, *34*, 1.
19. Bartell, F. E.; Smith, J. T. *J. Phys. Chem.* **1953**, *57*, 165.
20. Triambulo, R. E.; Cheong, H. G.; Lee, G. H.; Yi, I. S.; Park, J. W. *J. Alloy. Compd.* **2015**, *620*, 340.
21. Li, N.; Yang, G.; Sun, Y.; Song, H.; Cui, H.; Yang, G.; Wang, C. *Nano Lett.* **2015**, *15*, 3195.
22. Zhu, Y.; Qin, Q.; Xu, F.; Fan, F.; Ding, Y.; Zhang, T.; Wiley, B. J.; Wang, Z. L. *Phys. Rev. B, PRB* **2012**, *85*, 045443.
23. Johnston, I. D.; McCluskey, D. K.; Tan, C. K. L.; Tracey, M. C. *J. Micromech. Microeng.* **2014**, *24*, 457.
24. Schneider, F.; Fellner, T.; Wilde, J.; Wallrabe, U. *J. Micromech. Microeng.* **2008**, *18*, 065008.
25. Lu, N.; Wang, X.; Suo, Z.; Vlassak, J. *Appl. Phys. Lett.* **2007**, *91*, 221909.
26. Yu, Z. B.; Zhang, Q. W.; Li, L.; Chen, Q.; Niu, X. F.; Liu, J.; Pei, Q. B. *Adv. Mater.* **2011**, *23*, 664.
27. Ok, K. H.; Kim, J.; Park, S. R.; Kim, Y.; Lee, C. J.; Hong, S. J.; Kwak, M. G.; Kim, N.; Han, C. J.; Kim, J. W. *Sci. Rep.* **2015**, *5*, 1331.
28. Triambulo, R. E.; Park, J. W. *Curr. Appl. Phys.* **2015**, *15*, S12.